

DOI: <http://dx.doi.org/10.1590/1807-1929/agriambi.v27n10p772-778>

Energy performance of an agricultural articulated tractor: Manual and automatic modes¹

Desempenho energético de trator agrícola articulado: Modo manual versus automático

Gabriel G. Zimmermann^{2*}, Samir P. Jasper², Mariane C. da Costa²,
Gabriel A. de Oliveira² & Daniel Savi²

¹ Research developed at Universidade Federal do Paraná, Curitiba, PR, Brazil

² Universidade Federal do Paraná/Departamento de Solos e Engenharia Agrícola, Curitiba, PR, Brazil

HIGHLIGHTS:

Automatic mode presents less wheel slippage than manual mode at 4, 6, 8, and 10 km h⁻¹.

At 4 km h⁻¹, manual mode shows greater drawbar power and yield.

At lower speeds, automatic mode consumes less fuel per hour.

ABSTRACT: Automatic production management (APM) is a tool that assists in the operations of agricultural tractors, increasing yield and energy efficiency. The objective of the experiment was to compare the energy and operational performance of a 373-kW articulated tractor equipped with APM and manual mode of engine transmission and rotation, across different real-world speeds. The experiment was conducted in a randomized block design with five replicates, using a split-plot arrangement with two system modes (manual and automatic) in the plots and four real-world speeds (4, 6, 8, and 10 km h⁻¹) in the subplots, totaling 40 experimental units. The evaluated variables were: wheel slippage; engine rotation; hourly and specific fuel consumptions; drawbar force, power, and yield; operating speed; and engine thermal efficiency. The variance of the data was analyzed using Tukey's test for the first factor, and regression analysis for the second factor and interactions. The automatic mode showed lower engine rotation and wheel slippage without compromising the other variables. The use of this mode showed energy advantages at 4 and 6 km h⁻¹ by resulting in less fuel consumption per hour. In addition, the manual mode presented higher thermal efficiency at lower speeds than the automatic mode, which showed a linear increase.

Key words: engine rotation, fuel consumption, engine thermal efficiency

RESUMO: O gerenciamento automático de produtividade (APM) presente no trator agrícola é uma ferramenta importante que auxilia na operação, aumentando a eficiência e rendimento energético. O objetivo do experimento foi comparar o desempenho operacional e energético de um trator articulado de 373 kW equipado com APM e com o modo manual da transmissão e rotação do motor, sob diferentes velocidades reais. O experimento foi conduzido no delineamento de blocos casualizados em esquema de parcelas subdivididas, sendo as parcelas constituídas de dois modos de transmissão (manual e automático) e as subparcelas de quatro velocidades reais (4, 6, 8 e 10 km h⁻¹), com cinco repetições, totalizando 40 unidades experimentais. Foram monitorados a patinação dos rodados, rotação do motor, consumo horário e específico de combustível, força, potência e rendimento na barra de tração, velocidade operacional e eficiência térmica do motor. Os dados coletados foram submetidos à análise de variância, sendo o primeiro fator analisado pelo teste de Tukey, e o segundo fator e as interações por análise de regressão. No modo automático a rotação do motor e a patinação dos rodados foram menores sem comprometer as demais variáveis. Além disso, este modo, a 4 e 6 km h⁻¹, demonstrou uma vantagem energética, que requer menor consumo de combustível por hora. Além disso, o modo manual apresentou maior eficiência térmica em velocidades mais baixas quando comparado com o modo automático, que apresentou um aumento linear.

Palavras-chave: rotação do motor, consumo de combustível, eficiência térmica do motor

• Ref. 268548 – Received 10 Oct, 2022

* Corresponding author - E-mail: gabrielganancini@gmail.com

• Accepted 30 Apr, 2023 • Published 16 Jun, 2023

Editors: Ítalo Herbet Lucena Cavalcante & Carlos Alberto Vieira de Azevedo

This is an open-access article distributed under the Creative Commons Attribution 4.0 International License.



INTRODUCTION

The emergence of industrial-scale machinery and implements for agriculture in the last century has enabled significant productivity gains and operational performance improvements, definitively changing the trajectory of production techniques and increasing the supply of agricultural products (Kim et al., 2021), such as articulated tractors (Shafaei et al., 2022).

The automatic production management system (APM) used in current agricultural tractors (4WD) acts on the electronic transmission manager (gear ratio and engine speed), differing from the manual mode, in which the gear ratio is pre-set (Strapasson Neto et al., 2021). The use of embedded technologies for monitoring tractor performance, sensors that provide information on soil and crop conditions, and positioning systems have enabled efficient management of production processes. In this sense, the power-shift transmission (PST) integrates mechanics, control, and electronics to improve the efficiency of operations through a precise control of one or more pairs of shift clutches with the Transmission Control Unit (TCU). PST is commonly used in high horsepower tractors (4WD) to improve economy, operational efficiency, and dynamic performance (Wu et al., 2022). Therefore, in the current literature, most studies seek to evaluate the efficiency of PST only, which justifies experimental analyses of manual and automatic modes.

Thus, the objective of the experiment was to compare the energy and operational performance of a 373-kW articulated tractor equipped with APM and manual mode of engine transmission and rotation, across different real-world speeds.

MATERIAL AND METHODS

The experiment was performed in Pinhais, PR, Brazil, on a concrete surface, according to ASABE (2011a). A randomized block design in split-plot arrangement was used, with two system modes (G) (manual and automatic) in the plots, and four real-world speeds (S) (4, 6, 8, 10 km h⁻¹) in the subplots, totaling eight treatments. Each treatment had five replications, resulting in 40 experimental units (100 m long each). The automatic transmission and engine speed were performed simultaneously by the APM software, according to the real-world speed selected on the internal monitor of the cabin.

The tractor used in the study (Case IH™ Steiger 500) had a 4WD traction and a nominal power of 373 kW (ABNT, 2011) and was equipped with Full PowerShift transmission and an automatic production management (APM) system.

This tractor unit was used for both modes, considering the technology available. During the test, the set was equipped with Goodyear™ 710/70R42 double front and rear tires, with internal and external pressures of 68.95 and 82.74 kPa, respectively. The total weight of the tractor was 27,280 kg, with 61% distributed on the front axle and 39% on the rear axle, and the weight-to-power ratio was 73.14 kg kW⁻¹.

A convoy system was used in the experiment, in which the tractor pulled two other tractors (acting as a brake) by the drawbar (Figure 1): Steiger and Magnum models (Case IH™) with Full PowerShift transmission. Braking was performed by pre-set gear, providing 98 kN (10,000 kgf) as traction force, selected based on ASABE (2011b), considering a concrete surface and a tractor 4 × 4.

Throughout the experiment, a data acquisition system (DAS) consisting of a printed circuit board equipped with the sensors described below was used to collect data readings at a frequency of 1 Hz. The acquired data was then transferred to a hard disk for subsequent tabulation and analysis.

Wheel slippage was determined by engine rotation and tractor travel speed with and without load, according to Eq. 1.

$$WS = \left(1 - \frac{LTS \times UES}{UTS \times LES} \right) \times 100 \quad (1)$$

where:

- WS - wheel slippage, in %;
- LTS - loaded tractor speed, m s⁻¹;
- UTS - unloaded tractor speed, m s⁻¹;
- LES - loaded engine speed, rpm; and,
- UES - unloaded engine speed, rpm.

An encoder (model E100S, Autonics™) was used to acquire the engine speed (ES) from the power outlet (PO), and a digital tachometer (model DM6236P, Victor™) was used to obtain the transmission ratio ($R^2 = 0.99$).

An SVA-60 speed antenna (Agrosystem™) registered the operational speed (OS), quantifying the displacement as a function of the number of emitted pulses.

Two flowmeters (volumetric type - nutating disc; model RCDL25, BadgerMeter™) installed in the fuel supply system (tank inlet and return), measured the fuel consumption per hour (FCH). The difference in the number of pulses emitted by the flowmeters records the consumption and converts it into volume.

A load cell (Bermann™) was used to measure the drawbar force (DF), with a capacity of 300 kN, a sensitivity of 2.0 + 0.002

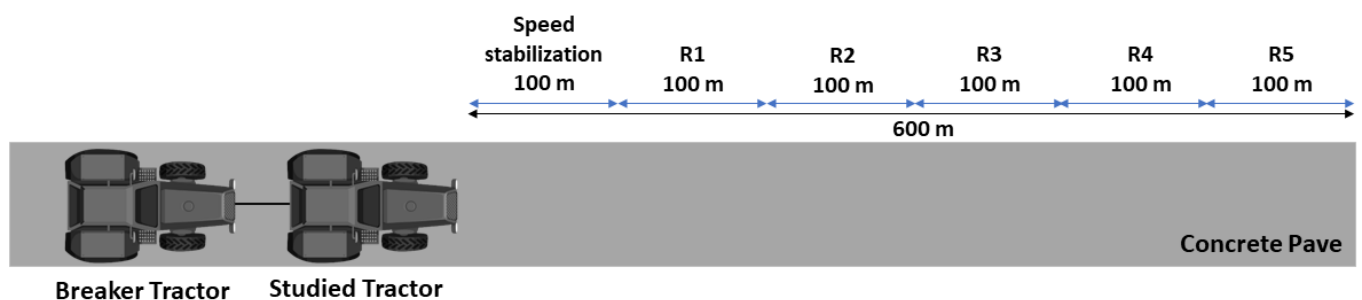


Figure 1. Experimental setup for evaluating the tractor operational performance on concrete paving

Mv V⁻¹, and an accuracy of 0.01 kN. Its calibration preceded the installation on the drawbar coupled to the tractor.

The power available in the drawbar as a function of force and speed was determined using Eq. 2.

$$DP = DF \times OS \quad (2)$$

where:

- DP - drawbar power, kW.
- DF - drawbar force, kN; and,
- OS - operational speed, m s⁻¹.

The drawbar yield was determined based on the power available in the drawbar and the tractor's engine, according to Eq. 3.

$$DY = \left(\frac{DP}{EP} \right) \times 100 \quad (3)$$

where:

- DY - drawbar yield, %;
- DP - drawbar power, kW; and,
- EP - engine power, kW.

Temperatures were measured by type K thermocouples that were installed next to the flowmeter in the fuel return. Temperature data were used to determine the diesel fuel density, according to Eq. 4.

$$D = (844.14 - 0.53) \times T \quad (4)$$

where:

- D - diesel fuel density, g L⁻¹;
- T - diesel fuel temperature, °C; and,
- 844.14 and 0.53 - density regression parameters.

Eq. 5 determined the mass-based fuel consumption per hour.

$$FCHM = \left(\frac{FCHV \times D}{1000} \right) \quad (5)$$

where:

- FCHM - fuel consumption per hour based on mass, g h⁻¹;

- FCHV - fuel consumption per hour based on volume, L h⁻¹;
- D - Diesel fuel density, g L⁻¹; and,
- 1000 - Conversion factor.

Eq. 6 determined the specific fuel consumption considering the mass-based consumption due to the power on the bar.

$$SFC = \left(\frac{FCHM}{DP} \right) \quad (6)$$

where:

- SFC - specific fuel consumption, g kW h⁻¹.

The engine thermal efficiency was obtained through specific consumption and lower calorific value of the fuel, using Eq. 7, according to Farias et al. (2017a).

$$ETE = \left(\frac{3600}{SFC \times LCV} \right) \quad (7)$$

where:

- ETE - engine thermal efficiency, %; and,
- LCV - lower calorific value, 42,295 MJ kg⁻¹.

The collected data were subjected to analysis of normality (Shapiro-Wilk test) and homogeneity of variance (Brown-Forsythe test). Significant means were subjected to analysis of variance to evaluate the effects of factors (G and S) and their interaction, using the statistical program Sigmaplot 12 (Systat Software™). When the F test was significant (p ≤ 0.05), the qualitative factor (G) means were compared using the Tukey's test (p ≤ 0.05), whereas the quantitative factor (S) means were compared using the regression test. The models were selected based on significance criteria (p ≤ 0.05) for the equation parameters and a higher coefficient of determination (R²).

RESULTS AND DISCUSSION

Table 1 contains the results from the analysis of variance and mean tests for the energy and operational performance data. Transforming the means for all studied variables was not necessary, denoting normality (Shapiro-Wilk) and homogeneity of variance residuals (Brown-Forsythe), except

Table 1. Summary of analysis of variance and the mean tests for the variables of energy and operational performance evaluated as a function of system modes (G) and real-world speeds (S)

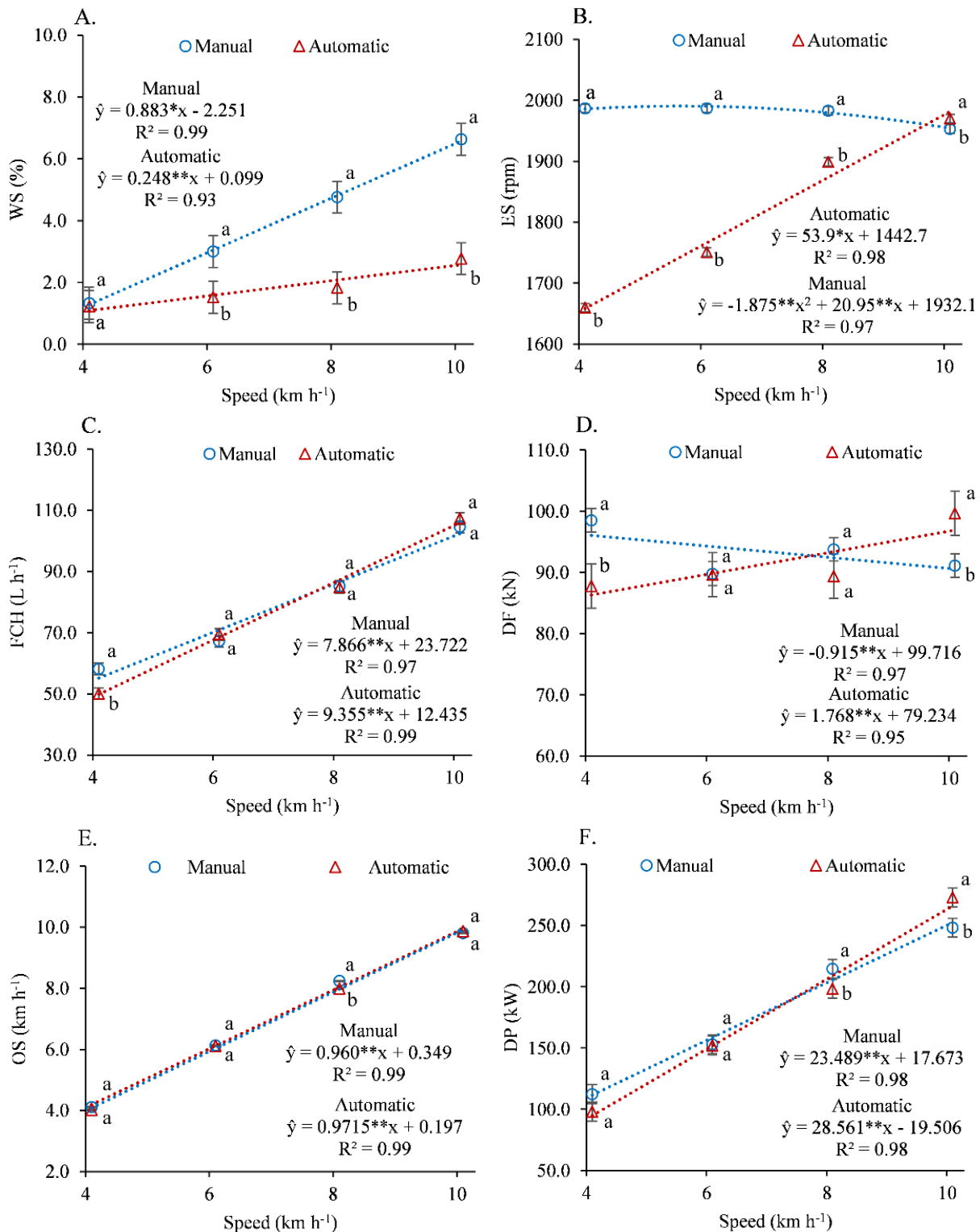
Analysis	Variables								
	WS (%)	ES (rpm)	FCH (L h ⁻¹)	DF (kN)	OS (km h ⁻¹)	DP (kW)	DY (%)	SFC (g kW h ⁻¹)	ETE (%)
Normality									
SW	0.26	0.51	0.86	0.06	0.11	0.33	0.22	0.35	0.87
Homogeneity									
BF	0.50	0.17	0.79	0.28	0.60	0.22	0.22	0.04	0.04
F Test									
G	225.91**	2,161**	0.94 ^{NS}	2.38 ^{NS}	5.23 ^{NS}	0.45 ^{NS}	0.45 ^{NS}	0.15 ^{NS}	0.37 ^{NS}
S	33.94**	4,721**	384.17**	1.75 ^{NS}	23.115**	264.78**	264.78**	42.19**	35.35**
G × S	19.12**	399.90**	10.80**	5.18*	3.52*	6.29**	6.29**	3.77*	4.64*

WS - Wheel slippage was determined by engine rotation and tractor travel speed with and without load, according to Eq. 1; ES - Engine speed; FCH - Fuel consumption per hour; DF - Drawbar force; OS - Operating speed; DP - Drawbar power; DY - Drawbar yield; SFC - Specific fuel consumption; and ETE - Engine thermal efficiency. Shapiro-Wilk normality test - SW ≤ 0.05 - Abnormal data; SW > 0.05 - Normal data. Analysis of homogeneity of variances by the Brown-Forsythe test - BF ≤ 0.05 - Heterogeneous variances; BF > 0.05 - Homogeneous variances. Analysis of variance (ANOVA) F-test: NS - Not significant; * - p ≤ 0.05 and ** - p ≤ 0.01. CV - Coefficient of variation

for specific fuel consumption (SFC) and engine thermal efficiency (ETE), which provided heterogeneous dynamics. The coefficient of variation for all variables was stable, except for wheel slippage (WS), which presented an average dispersion for all factors analyzed, according to Ferreira (2018).

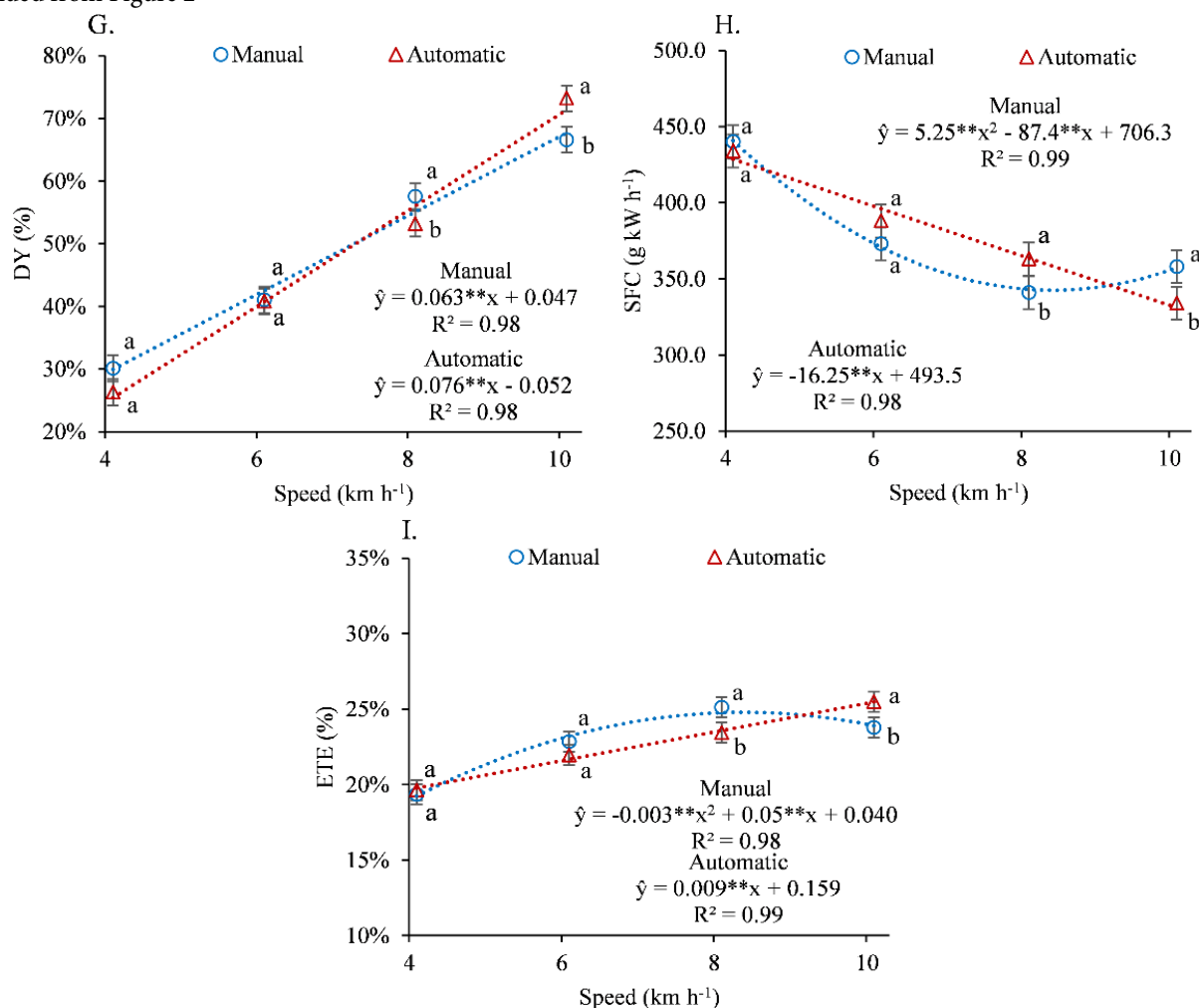
The system modes showed a significant difference in the variables WS and engine speed (ES). The stability of the tensile force demanded during the treatments was found for the speed factor, as the only non-significant variable was the drawbar force (DF). The interaction between modes and real-world speed showed differences for all variables.

The automatic system presents less wheel slippage than the manual at 6, 8, and 10 km h⁻¹ (Figure 2A). This is due to the APM functionality, which processes the parameters and, when necessary, readjusts its strategy, which corroborates the dynamics observed in the engine rotation. This indicates that the selected speed affects WS (Monteiro et al., 2011). The manual mode showed a better fit with the ideal range (4 to 8%) proposed by ASABAE (2011a) for concrete surface operations. Contrastingly, the automatic mode presented an overload on the powertrain (Battiato & Diserens, 2017); this overload can be attributed



Continued on the next page

Continued from Figure 2



* - Significant at $p \leq 0.05$ and ** - significant at $p \leq 0.01$ by the F test; Vertical bar - Minimum significant difference (MSD). Symbols followed by the same lowercase letter do not differ from each other by the Tukey's test ($p \leq 0.05$)

Figure 2. Wheel- slippage - WS (A), engine speed - ES (B), Fuel consumption per hour - FCH (C), drawbar force- DF (D), operating speed - OS (E), drawbar power - DP (F), drawbar yield - DY (G), specific fuel consumption - SFC (H) and engine thermal efficiency - ETE (I) as a function of real-world speeds

to the operational principle of the transmission, which is dependent on engine speed.

Regarding ES (Figure 2B), the manual mode expressed a second-order polynomial trend. The maximum engine rotation of 1990 rpm corresponds to a tractor speed of 5.58 km h⁻¹. Contrastingly, the automatic system presented an increase proportional to the speed, showing the highest ES at 10 km h⁻¹. The higher engine speed shown in the manual mode at 4, 6, and 8 km h⁻¹ is due to the maintenance of the selected target rotation. In the APM, the ES shifts according to the applied load and it is not constant, as in the manual mode where the target rotation is set beforehand by the operator, as found by Strapasson Neto et al. (2021). The increase in the automatic mode is more gradual due to the technology's dynamics, which maintains the engine speed between gear shifts with a subtle increment.

Fuel consumption per hour (Figure 2C) increased as the speed increased, not significantly differing between modes at speeds of 6, 8, and 10 km h⁻¹, and expressing difference at 4 km h⁻¹. Higher fuel consumption at higher speeds is due to the use of higher gears, resulting in higher effective speed. It denotes an energy advantage for the automatic mode at

4 km h⁻¹, consuming 8.08 L h⁻¹ less fuel than the manual mode at this speed.

DF presented a linear increase in the automatic mode (Figure 2D) due to the constant adjustment of the APM with the load. This adjustment occurs as a function of the increase in ES and its conversion into operating speed, as highlighted by Lopes et al. (2010) and Zimmermann et al. (2022). Regarding the manual system, DF decreased with increasing load demand, reducing the rotation.

According to the mean tests, DF did not show significant differences at 6 and 8 km h⁻¹, resulting in equivalent loads despite the different dynamics due to the increases in real-world speeds. The operational speed (Figure 2E) in both modes had a similar linear trend, differing only at 8 km h⁻¹, for which the manual mode had better performance. This may be due to the slippage of the wheelsets and the occurrence of alternations in the moment of load on the engine (Damanauskas & Janulevičius, 2015). Balsari et al. (2021) highlighted the importance of this variable for understanding the relationship between transmission and operational efficiency. The analysis of the interaction between factors and drawbar power (DP) and drawbar yield (DY) (Figures 2F and G) showed an

increasing linear trend of energy availability in the drawbar, at expense of speed, in both modes. No significant difference was found between the modes at speeds of 4 and 6 km h⁻¹. The manual mode was superior by 16 kW at 8 km h⁻¹, and the automatic by 24.70 kW at 10 km h⁻¹. This is explained by the transmission architecture combined with the gradual and constant increases in ES and operating speed (OS) at these speeds, resulting in increases in DY. SFC (Figure 2H) showed a second-order polynomial trend for the manual mode and a linear trend for the automatic mode, denoting significant gains in energy performance when operating at higher speed and, consequently, higher traction load. The manual and automatic modes did not differ at 4 and 6 km h⁻¹, but the manual mode was more efficient in fuel consumption (342.54 g kW h⁻¹) at 8 km h⁻¹, whereas the automatic mode was more efficient (331 g kW h⁻¹) at 10 km h⁻¹. This phenomenon occurs because APM mode optimizes both engine performance and traction efficiency simultaneously with the increase in speed (Cutini et al., 2022), whereas the manual mode showed a trend of increasing fuel consumption at 10 km h⁻¹. The decrease in specific fuel consumption denoted greater utilization during the transformation of the chemical energy contained in fuels into work (Farias et al., 2017b). The automatic mode showed a linear increase in engine thermal efficiency (Figure 2I) at higher speeds (25.45% at 10.0 km h⁻¹), differing from the manual mode, which showed the highest ETE (24.88%) at 8.33 km h⁻¹. This is due to the greater thermal efficiency occurring when rotations are close to the maximum torque regime and higher speeds, reducing fuel consumption, according to Serrano et al. (2007) and Ince & Güler (2020). Despite the previously described difference in operation, no significant difference was found between the transmission modes at 4 and 6 km h⁻¹, which can be explained by the lower effect of ES and OS on the engine thermal efficiency.

CONCLUSIONS

1. The use of automatic production management resulted in lower values of engine rotation and wheel slippage, with no significant differences for the other variables.
2. The automatic mode showed an energy advantage at 4 and 6 km h⁻¹ by presenting less fuel consumption per hour.
3. The manual mode presented higher thermal efficiency at lower speeds when compared to the automatic mode, which showed a linear increase.

LITERATURE CITED

- ABNT - Brazilian Technical Standards Association. ISO TR14396. Reciprocating internal combustion engines - Determination and method for measuring engine power. Rio de Janeiro, 2011. 10p.
- ASABE - American Society of Agricultural Biological Engineers. ASABE 496.3. Agricultural machinery management data. St. Joseph, 2011a. 6p.
- ASABE - American Society of Agricultural Biological Engineers. ASABE 497.7. Agricultural machinery management data. St. Joseph, 2011b. 33p.
- Balsari, P.; Biglia, A.; Comba, L.; Sacco, D.; Alcatrao, L. E.; Varani, M.; Mattetti, M.; Barge, P.; Tortia, C.; Manzone, M.; Gay, P.; Aimonino, D. R. Performance analysis of a tractor-power harrow system under different working conditions. *Biosystems Engineering*, v.202, p.28-41, 2021. <https://doi.org/10.1016/j.biosystemseng.2020.11.009>
- Battiatto, A.; Diserens, E. Tractor traction performance simulation on differently textured soils and validation: A basic study to make traction and energy requirements accessible to the practice. *Soil and Tillage Research*, v.66, p.18-32, 2017. <https://doi.org/10.1016/j.still.2016.09.005>
- Cutini, M.; Brambilla, M.; Pochi, D.; Fanigliulo, R.; Bisaglia, C. A Simplified Approach to the Evaluation of the Influences of Key Factors on Agricultural Tractor Fuel Consumption during Heavy Drawbar Tasks under Field Conditions. *Agronomy*, v.12, p.1-15, 2022. <https://doi.org/10.3390/agronomy12051017>
- Damanauskas, V.; Janulevičius, A. Differences in tractor performance parameters between single-wheel 4WD and dual-wheel 2WD driving systems. *Journal of Terramechanics*, v.60, p.63-73, 2015. <https://doi.org/10.1016/j.jterra.2015.06.001>
- Farias, M. S. de; Schlosser, J. F.; Linares, P.; Barbieri, J. P.; Negri, G. M.; Oliveira, L. F. V. de; Rüdell, P. Efficiency in fuel consumption of an agricultural tractor equipped with continuously variable transmission. *Ciência Rural Magazine*, v.47, p.1-8, 2017a.
- Farias, M. S. de; Schlosser, J. F.; Martini, A. T.; Santos, G. O. dos; Estrada, J. S. Air and fuel supercharge in the performance of a diesel cycle engine. *Ciência Rural Magazine*, v.47, p.1-7, 2017b. <https://doi.org/10.1590/0103-8478cr20161117>
- Ferreira, P.V. Experimental statistics applied to agricultural sciences. Viçosa: UFV, 2018. 126p.
- Ince, E.; Güler, M. A. On the advantages of the new power-split infinitely variable transmission over conventional mechanical transmissions based on fuel consumption analysis. *Journal of Cleaner Production*, v.244, p.1-14, 2020. <https://doi.org/10.1016/j.jclepro.2019.118795>
- Kim, W-S.; Kim, Y-J.; Park, S-U.; Kim, Y-S. Influence of soil moisture content on the traction performance of a 78-kW agricultural tractor during plow tillage. *Soil and Tillage Research*, v.207, p.1-12, 2021. <https://doi.org/10.1016/j.still.2020.104851>
- Lopes, A.; Câmara, F. T. da; la Scala Júnior, N.; Furlani, C. E. A.; Silva, R. P. da; Barbosa, A. L. P. B. Performance of an "aerosol" prototype. *Agricultural Engineering*, v.30, p.82-91, 2010. <https://doi.org/10.1590/S0100-69162010000100009>
- Monteiro, L. de A.; Lanças, K. P.; Guerra, S. P. S. Desempenho de um trator agrícola equipado com pneus radiais e diagonais com três níveis de lastros líquidos. *Agricultural Engineering*, v.31, p.551-560, 2011. <https://doi.org/10.1590/S0100-69162011000300015>
- Serrano, J. M.; Peça, J. O.; Silva, J. M. da; Pinheiro, A.; Carvalho, M. Tractor energy requirements in disc harrow systems. *Biosystems Engineering*, v.98, p.286-296, 2007. <https://doi.org/10.1016/j.biosystemseng.2007.08.002>
- Shafaei, S. M.; Loghavi, M.; Kamgar, S. An Experimental Investigation of Drawbar Pull Performance of Front Wheel Assist Tractors. *Transactions of the Indian National Academy of Engineering*, v.7, p.1369-1380, 2022. <https://doi.org/10.1007/s41403-022-00370-y>

- Strapasson Neto, L.; Jasper, S. P.; Kmiecik, L. L.; Silva, T. X. da; Savi, D. Performance of agricultural tractor with and without automatic transmission and engine rotation management. *Revista Brasileira de Engenharia Agrícola e Ambiental*, v.25, p.498-502, 2021. <https://doi.org/10.1590/1807-1929/agriambi.v25n7p498-502>
- Strapasson Neto, L.; Kmiecik, L. L.; Jasper, S. P.; Zimmermann, G. G.; Savi, D. Interference of the number of remote control valves in use on the energy performance of an agricultural tractor with productivity management. *Engenharia Agrícola*, v.40, p.356-362, 2020. <http://dx.doi.org/10.1590/1809-4430-Eng.Agric.v40n3p356-362/2020>
- Wu, Y.; Mao, Y.; Xu, L. FMI-based co-simulation method and test verification for tractor power-shift transmission. *Plos one*, v.17, p.1-14, 2022. <https://doi.org/10.1371/journal.pone.0263838>
- Zimmermann, G. G.; Savi, D.; Jasper, S. P.; Kmiecik, L. L.; Strapasson Neto, L.; Sobenko, L. R. Energy performance of farm tractor with single radial versus dual diagonal wheels in harrowing operations. *Revista Brasileira de Engenharia Agrícola e Ambiental*, v.26, p.356-364, 2022. <https://doi.org/10.1590/1807-1929/agriambi.v26n5p356-364>